Supplementary information

Co(III) Corroles with Pendant Amidophenol and Amidopyridine Substituents Facilitates Electrocatalytic Hydrogen Evolution Reaction via Second Coordination Sphere Effects

Xu-You Cao,[a] Shi-Yin Xu,[a] Ling-Wei Wu,[a] Yi-Feng Qiu,[a] Hao Zhang,[a] Li-Ping Si,[a,b]* Li-Ming Wang[a] and Hai-Yang Liu,[a]*

[a] School of Chemistry and Chemical Engineering, Guangdong Provincial Key Laboratory of Fuel Cell Technology, South China University of Technology, Guangzhou 510641, China.

[b] School of Materials Science and Energy Engineering, Foshan University, Foshan 528000, PR China

*Correspondence: chhyliu@scut.edu.cn (H.-Y. Liu).

Table of content

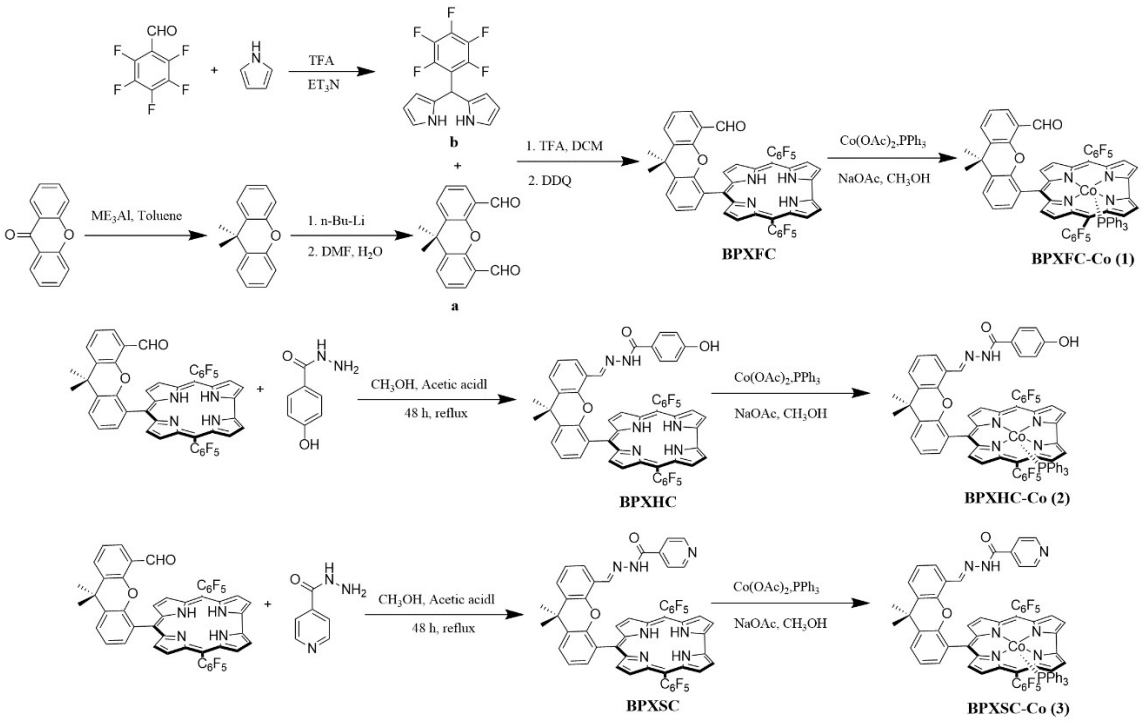

Scheme S1. The synthetic route of Co corrole complexes **1-3**.

Synthesis of a.

9,9-Dimethylxanthene (5 g, 23.78 mmol) was added to a dried 500 mL three-necked flask, evacuated and protected by nitrogen filling. Then 160 mL of dry hexane was added for stirring, followed by tetramethylethylenediamine (9 mL, 60 mmol). Subsequently n-butyllithium (n-hexane 1.6 mol, 45 mL, 71.34 mol) was added slowly dropwise over 30 min, and after completion of the dropwise addition the reaction mixture was refluxed for 15 min and cooled to room temperature. Then dry 10 mL DMF was slowly added and stirring was continued for 1 hour. At the end of the reaction, the reaction mixture was transferred to an ice bath, the reaction was quenched with excess HCl/H_2O, and the white solid formed was collected by vacuum filtration and dried under vacuum. The complex **a** did not require purification and could be used directly in the next step of the experiment.

Synthesis of b.

Pentafluorobenzaldehyde (2.8 g, 14.28 mmol) was added to 160 mL of freshly evaporated pyrrole with stirring and 120 μL of trifluoroacetic acid (TFA) was added as a catalyst and the

reaction was carried out for 1 h at room temperature. At the end of the reaction, 240 μL of ethylenediamine was added to burst the reaction. The excess pyrrole was subsequently evaporated out by distillation under reduced pressure at 130 °C to obtain an oily crude product. The crude product was purified by silica gel column chromatography (V_{Hex}/V_{DCM} = 1:1) and used directly in the next experiment.

Synthesis of BPXFC.

a (0.2663 g, 1 mmol) and **b** (0.7806 g, 2.5 mmol) were dissolved in dried 780 mL DCM, followed by the addition of 60 μL of trifluoroacetic acid (TFA) as a catalyst, and shading and stirring at room temperature overnight. Then 120 μL of ethylenediamine was added to neutralize the trifluoroacetic acid, and then DDQ (0.454 g, 2 mmol) was added to continue the reaction under the shade for one hour. The reaction was finished after one hour, and the solvent was removed by spin evaporation. The crude product was purified by silica gel column chromatography (V_{Hex}/V_{DCM} = 5:1→3:1) to afford purple solids of **BPXFC** (102 mg, yield 11.7%).^{1}H NMR (400 MHz, Chloroform-d) δ 9.12 (d, J = 4.3 Hz, 2H), 8.66 (s, 4H), 8.57 (d, J = 4.3 Hz, 2H), 7.98 (dd, J = 7.4, 1.6 Hz, 1H), 7.91 (dd, J = 8.0, 1.6 Hz, 1H), 7.76 – 7.70 (m, 2H), 7.58 (t, J = 7.6 Hz, 1H), 7.35 (dd, J = 7.7, 1.6 Hz, 1H), 7.07 (t, J = 7.7 Hz, 1H), 1.92 (s, 6H). ^{19}F NMR (376 MHz, Chloroform-d) δ -137.03 – -137.20 (m), -137.98 (d, J = 24.1 Hz), -152.91 (t, J = 21.2 Hz), -161.40 – -161.72 (m), -161.95 (t, J = 22.2 Hz). HRMS (ESI) $[M + H]^+$, calculated for $C_{47}H_{25}F_{10}N_4O_2$: 867.1833, found: 867.1812.

Synthesis of BPXHC

BPXFC (0.1 g, 0.115 mmol) and 4-hydroxybenzoyl hydrazine (0.0875 g, 0.575 mmol) were dissolved in 50 mL of methanol, and 0.5 g of anhydrous sodium sulfate was added as a dehydrate, and heated and stirred at reflux for 48 hours. After ending the reaction, the solvent was removed by spin evaporation. The crude product was purified by silica gel column chromatography (V_{DCM}/V_{EA} = 10:1→4:1) to afford a blue-green solid **BPXHC** (101 mg, yield 87.72%).^{1}H NMR (400 MHz, DMSO-d6) δ 9.94 (s, 1H), 9.33 (d, J = 4.3 Hz, 2H), 8.89 (d, J =

4.7 Hz, 2H), 8.78 (s, 2H), 8.52 (d, J = 4.7 Hz, 2H), 8.29 (s, 1H), 8.09 – 7.98 (m, 2H), 7.73 – 7.59 (m, 2H), 7.55 (d, J = 7.7 Hz, 1H), 7.12 (t, J = 7.7 Hz, 1H), 6.10 (d, J = 8.1 Hz, 2H), 5.76 (d, J = 8.1 Hz, 2H), 5.61 (s, 1H), 1.86 (s, 6H). ^{19}F NMR (376 MHz, DMSO-d6) δ -139.42 (d, J = 144.4 Hz), -154.77, -162.82 (dd, J = 42.1, 22.0 Hz). HRMS (ESI) $[M + H]^+$, calculated for $C_{54}H_{31}F_{10}N_6O_3$: 1001.2292, found: 1001.2325.

Synthesis of BPXSC

BPXFC (0.1 g, 0.115 mmol) and isoniazid (0.078 g, 0.575 mmol) were dissolved in 50 mL of methanol, and 0.5 g of anhydrous sodium sulfate was added as a dewatering agent, stirred, and heated to reflux for 48 hours. After ending the reaction, the solvent was removed by spin evaporation. The crude product was purified by silica gel column chromatography (V_{DCM}/V_{EA} = 10:1→5:1) to afford a blue solid **BPXSC** (97 mg, yield 87.12%).^{1}H NMR (400 MHz, DMSO-d6) δ 9.33 (d, J = 4.3 Hz, 2H), 8.89 (d, J = 5.0 Hz, 2H), 8.73 (d, J = 4.3 Hz, 2H), 8.57 – 8.45 (m, 3H), 8.04 (dd, J = 24.9, 6.3 Hz, 4H), 7.73 (dd, J = 7.7, 1.6 Hz, 1H), 7.67 (t, J = 7.7 Hz, 1H), 7.54 (dd, J = 7.8, 1.5 Hz, 1H), 7.15 (t, J = 7.7 Hz, 1H), 5.70 (d, J = 5.6 Hz, 2H), 5.61 (s, 1H), 1.86 (s, 6H). ^{19}F NMR (376 MHz, DMSO-d6) δ -139.61, -154.80, -162.85 (q, J = 29.8, 27.6 Hz). HRMS (ESI) $[M + H]^+$, calculated for $C_{37}H_{21}F_5N_4O_2$: 986.2296, found: 986.2322.

Synthesis of BPXFC-Co（1）

BPXFC (50 mg, 57.5 μ mol), anhydrous sodium acetate (113.64 mg, 1.385 mmol) and triphenylphosphine (190 mg, 724 μmol) were dissolved in 10 mL of methanol and 10 m of dichloromethane, then Co acetate tetrahydrate (113.64 mg, 456 μmol) was added for stirring, and the reaction was shrouded from the light for one hour. At the end of the reaction, it was extracted with water and dichloromethane, the organic phase was collected and dried with Na_2SO_4, and the solvent was removed by spin distillation. The crude product was purified by silica gel column chromatography (V_{Hex}/V_{DCM} =3:1) to afford a purple-red solid **BPXFC-Co** (56 mg, yield 82.17%).^{1}H NMR (400 MHz, Chloroform-d) δ 8.74 (d, J = 4.6 Hz, 2H), 8.22 (q,

J = 5.0 Hz, 4H), 8.05 (d, J = 4.5 Hz, 2H), 7.82 (d, J = 7.8 Hz, 1H), 7.71 (s, 1H), 7.69 – 7.61 (m, 1H), 7.44 – 7.35 (m, 2H), 7.09–7.00 (m, 4H), 6.69 (td, J = 7.8, 2.5 Hz, 6H), 4.65 (dd, J = 11.2, 7.8 Hz, 6H), 1.84 (s, 6H). ^{19}F NMR (376 MHz, Chloroform-d) δ -135.87 (d, J = 24.3 Hz), -137.98 (d, J = 24.7 Hz), -154.31 (t, J = 21.1 Hz), -161.77 (t, J = 22.7 Hz), -162.82 (t, J = 23.0 Hz). HRMS (ESI) $[M + H]^+$, calculated for $C_{65}H_{37}CoF_{10}N_4O_2P$: 1185.1821, found: 1185.1835.

Synthesis of BPXHC-Co（2）

BPXHC-Co was prepared in the same way as **BPXFC-Co**, and the crude product was purified by silica gel column chromatography (V_{DCM}/V_{EA} =5:1) to obtain **BPXHC-Co** (65 mg, yield 84.24%) as a red solid. ^{1}H NMR (400 MHz, DMSO-d^6) δ 9.75 (s, 1H), 9.03 (s, 1H), 8.95 (s, 2H), 8.49 (d, J = 5.0 Hz, 2H), 8.27 (d, J = 4.4 Hz, 2H), 8.21 (d, J = 4.8 Hz, 2H), 7.99 (d, J = 6.3 Hz, 1H), 7.68 (d, J = 6.2 Hz, 1H), 7.66 – 7.51 (m, 2H), 7.46 (d, J = 7.6 Hz, 1H), 7.23 (s, 1H), 7.14 (d, J = 3.5 Hz, 3H), 6.78 (s, 6H), 6.09 (s, 1H), 6.00 (d, J = 7.6 Hz, 2H), 5.87 – 5.76 (m, 2H), 4.54 (s, 6H), 1.83 (s, 6H). ^{19}F NMR (376 MHz, DMSO-d6) δ -138.39 (dd, J = 287.4, 25.7 Hz), -155.05 (t, J = 22.5 Hz), -162.78 (dt, J = 139.9, 22.5 Hz). HRMS (ESI) $[M + Na]^+$, calculated for $C_{72}H_{42}CoF_{10}N_6NaO_3P$: 1341.2120, found: 1341.2132.

Synthesis of BPXSC-Co（3）

BPXSC-Co was prepared in the same way as **BPXFC-Co**. The crude product was purified by silica gel column chromatography (V_{DCM}/V_{EA} =4:1) to obtain **BPXSC-Co** (53 mg, yield 70.96%) as a deep purple solid. ^{1}H NMR (400 MHz, DMSO-d_6) δ 8.48 (s, 2H), 8.19 (s, 4H), 7.99 (d, J = 8.0 Hz, 1H), 7.71 (d, J = 7.8 Hz, 1H), 7.63 (ddd, J = 10.4, 6.4, 2.2 Hz, 4H), 7.59 – 7.44 (m, 6H), 7.19 – 7.07 (m, 5H), 6.74 (s, 6H), 4.48 (s, 6H), 1.81 (s, 6H). ^{19}F NMR (376 MHz, DMSO-d_6) δ -138.54 (d, J = 141.0 Hz), -155.05 (t, J = 22.5 Hz), -162.80 (d, J = 106.9 Hz). HRMS (ESI) $[M + H]^+$, calculated for $C_{71}H_{42}CoF_{10}N_7O_2P$: 1304.2304, found: 1304.2321.

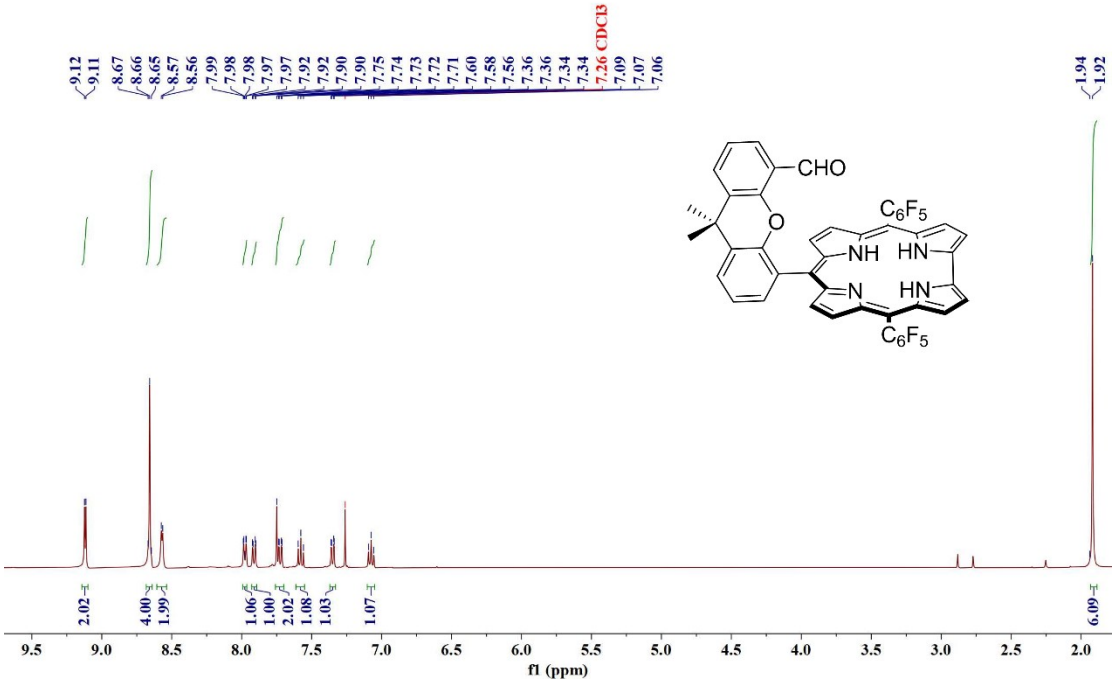

Fig. S1-1 ^{1}H NMR spectrum of **BPXFC** .

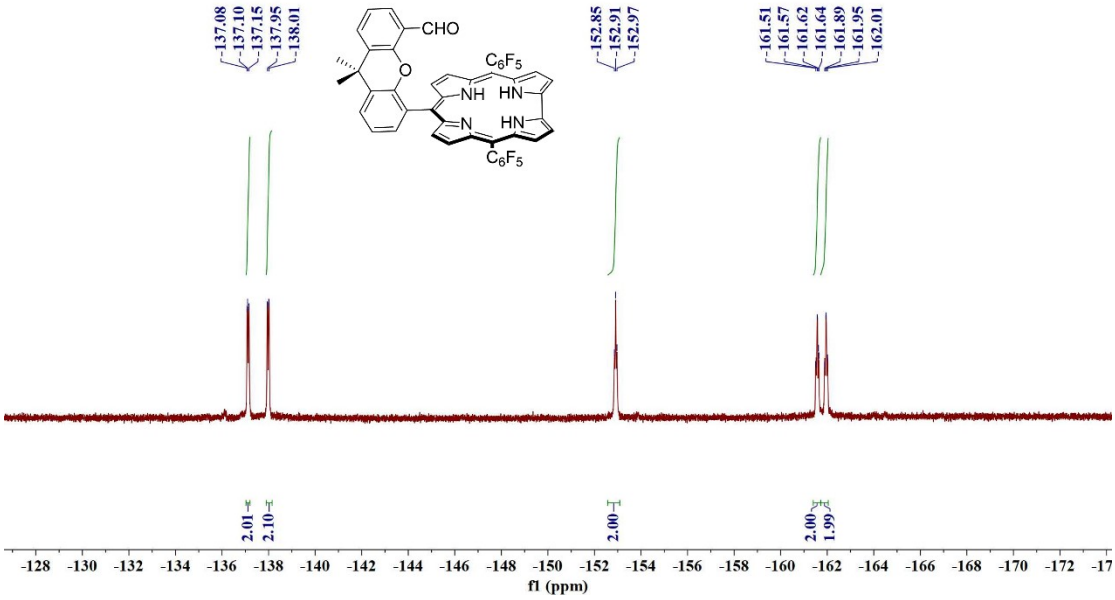

Fig. S1-2 ^{19}F NMR spectrum of **BPXFC**.

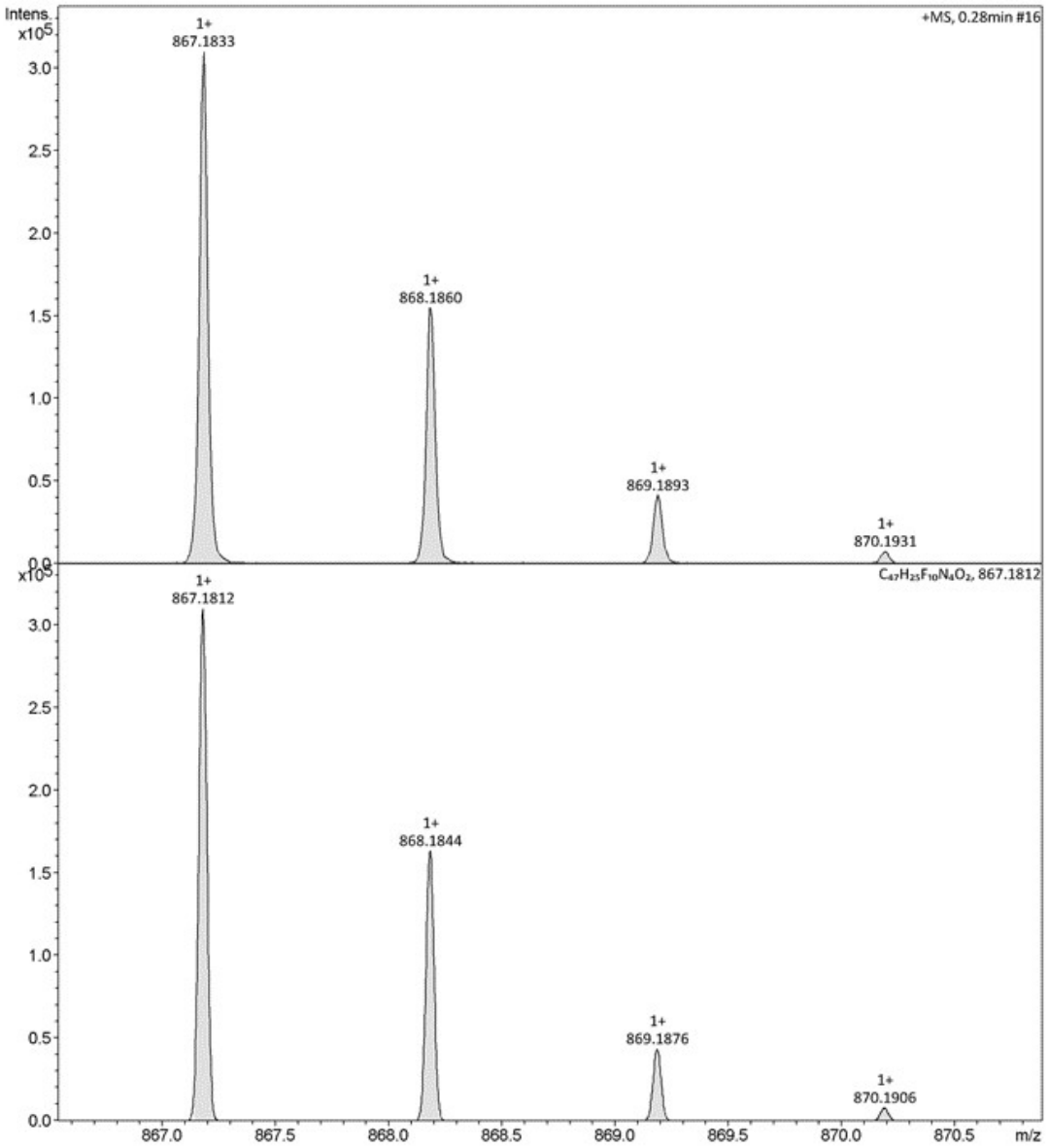

Fig. S1-3 ESI-HRMS spectrum of **BPXFC**.

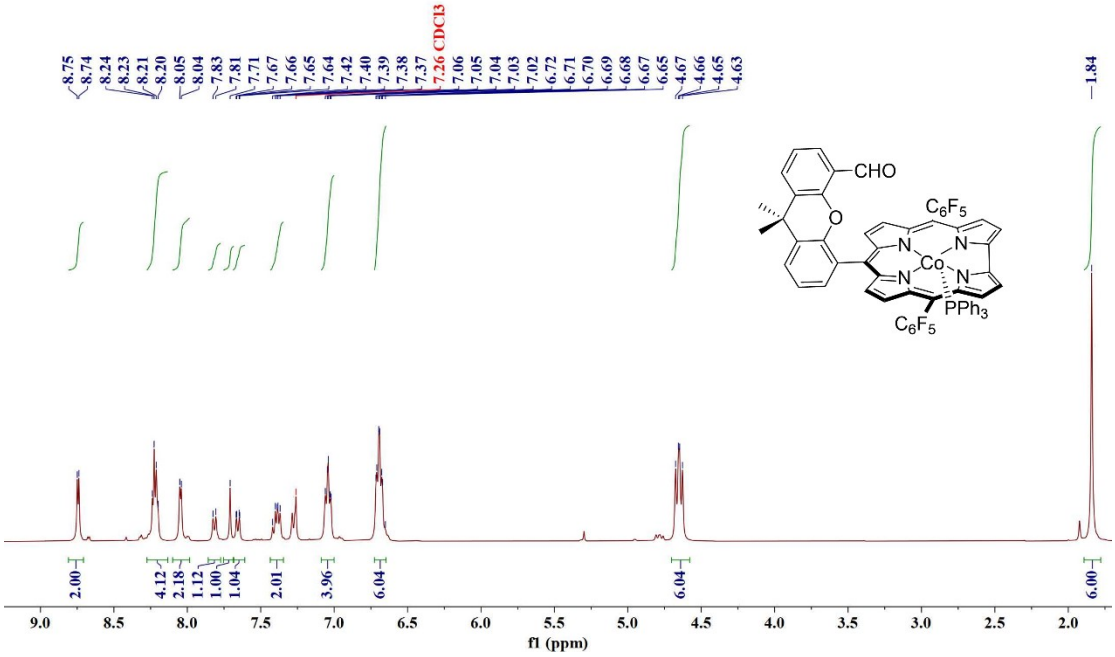

Fig. S2-1 ^{1}H NMR spectrum of **BPXFC-Co (1)**.

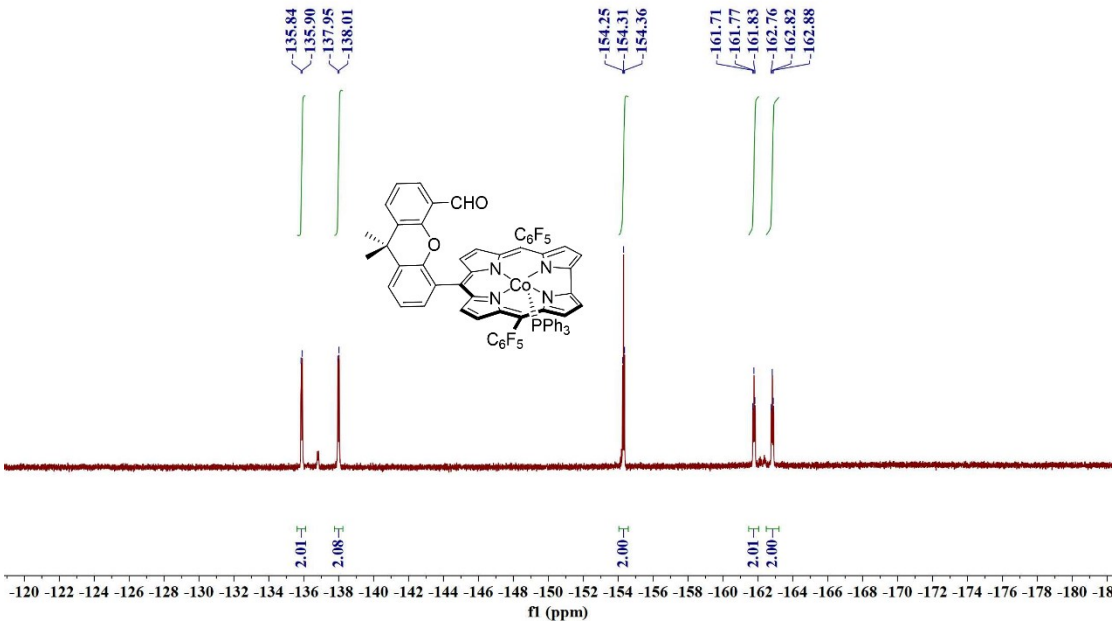

Fig. S2-2 ^{19}F NMR spectrum of **BPXFC-Co (1)**.

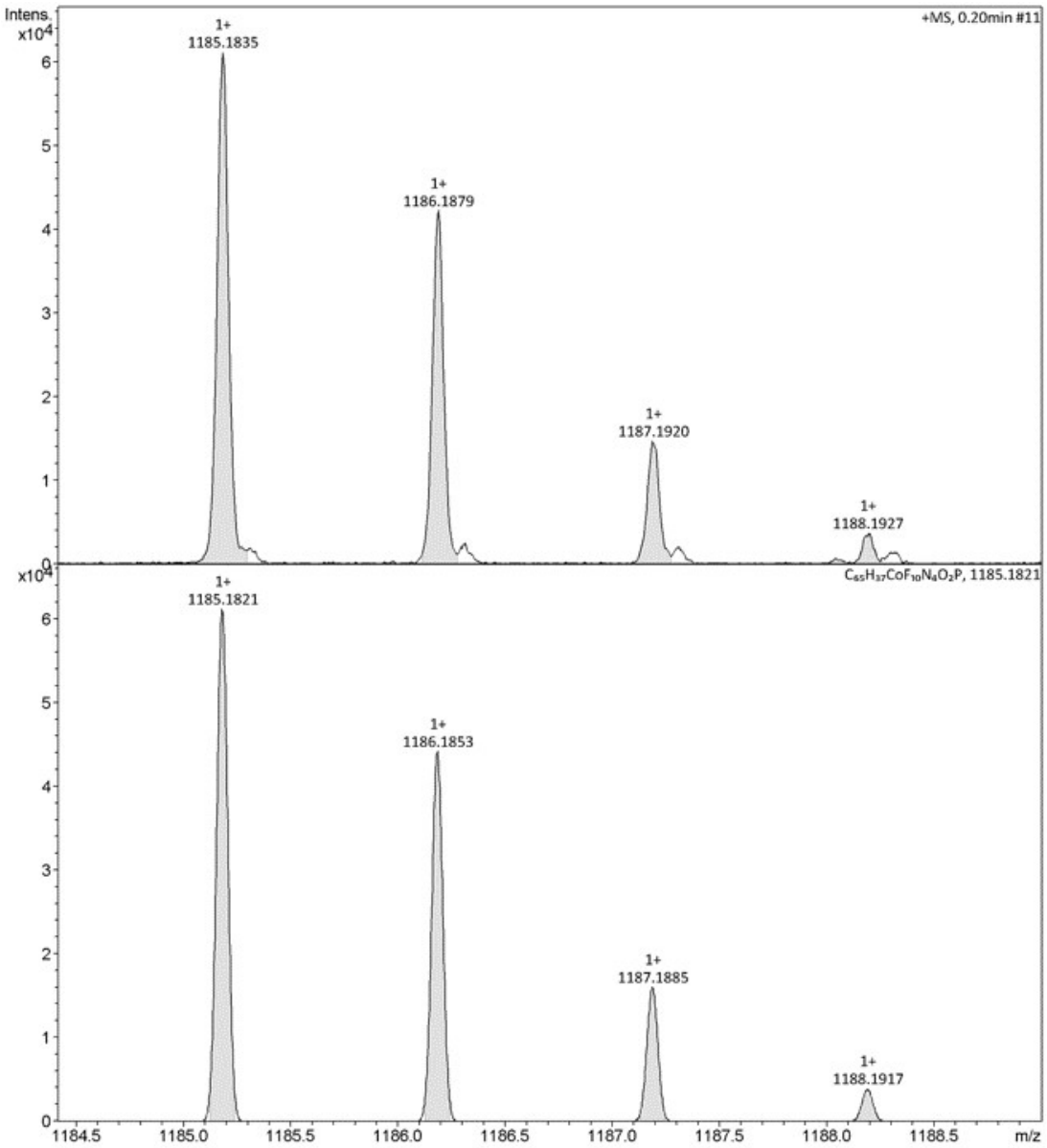

Fig. S2-3 ESI-HRMS spectrum of **BPXFC-Co (1)**.

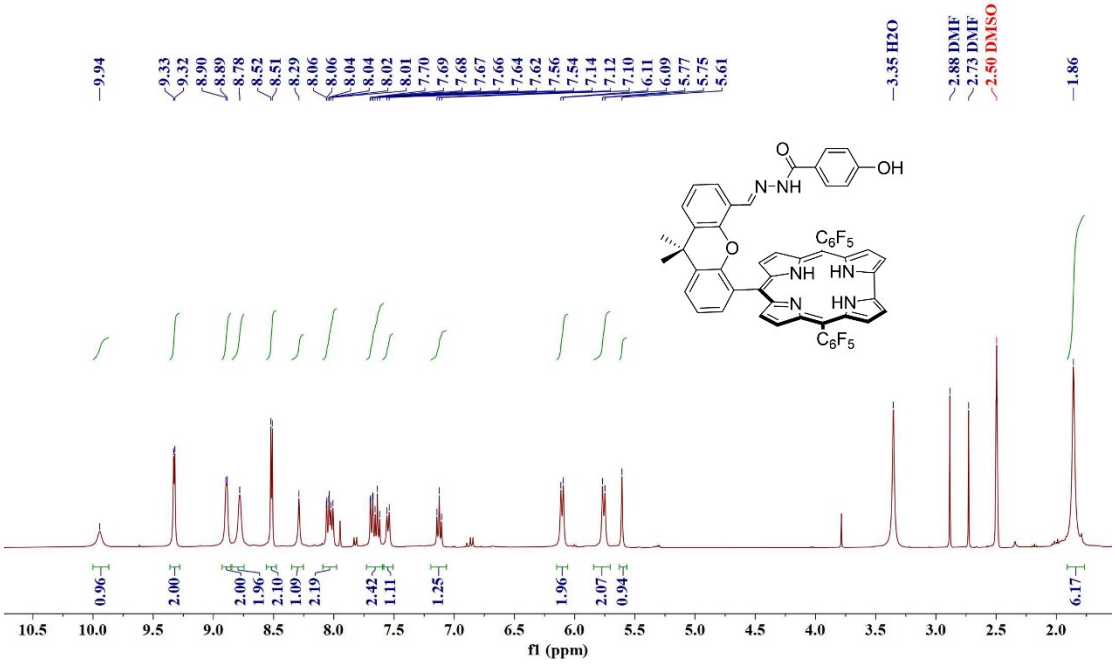

Fig. S3-1 ^{1}H NMR spectrum of **BPXHC**.

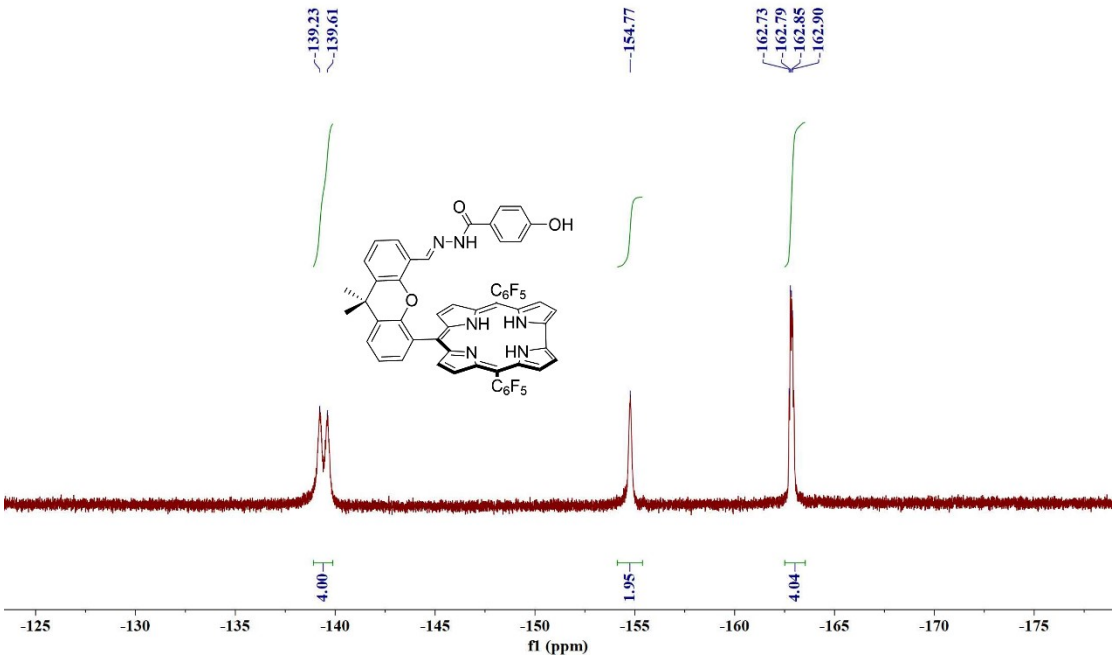

Fig. S3-2 ^{19}F NMR spectrum of **BPXHC**.

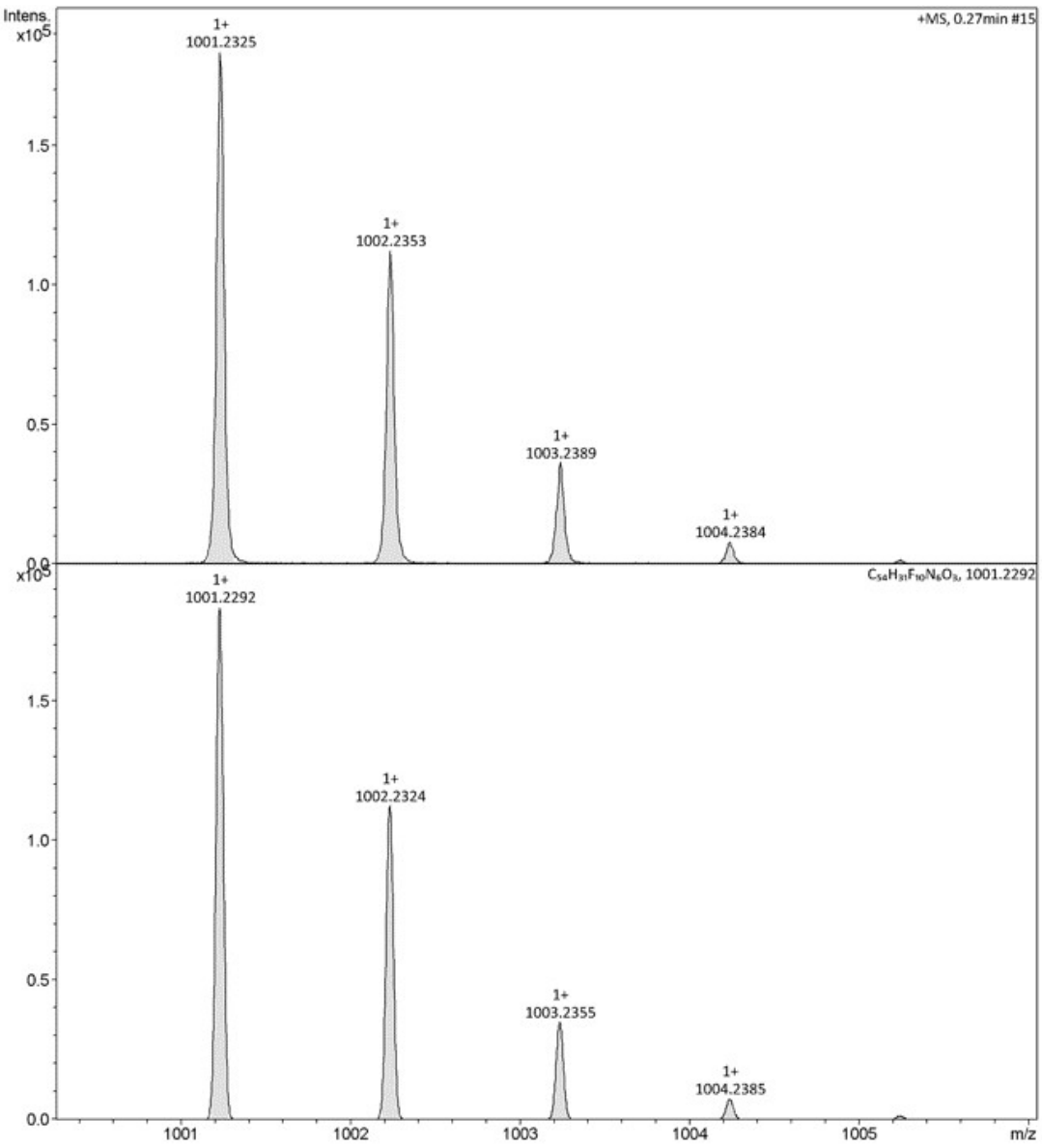

Fig. S3-3 ESI-HRMS spectrum of **BPXHC**.

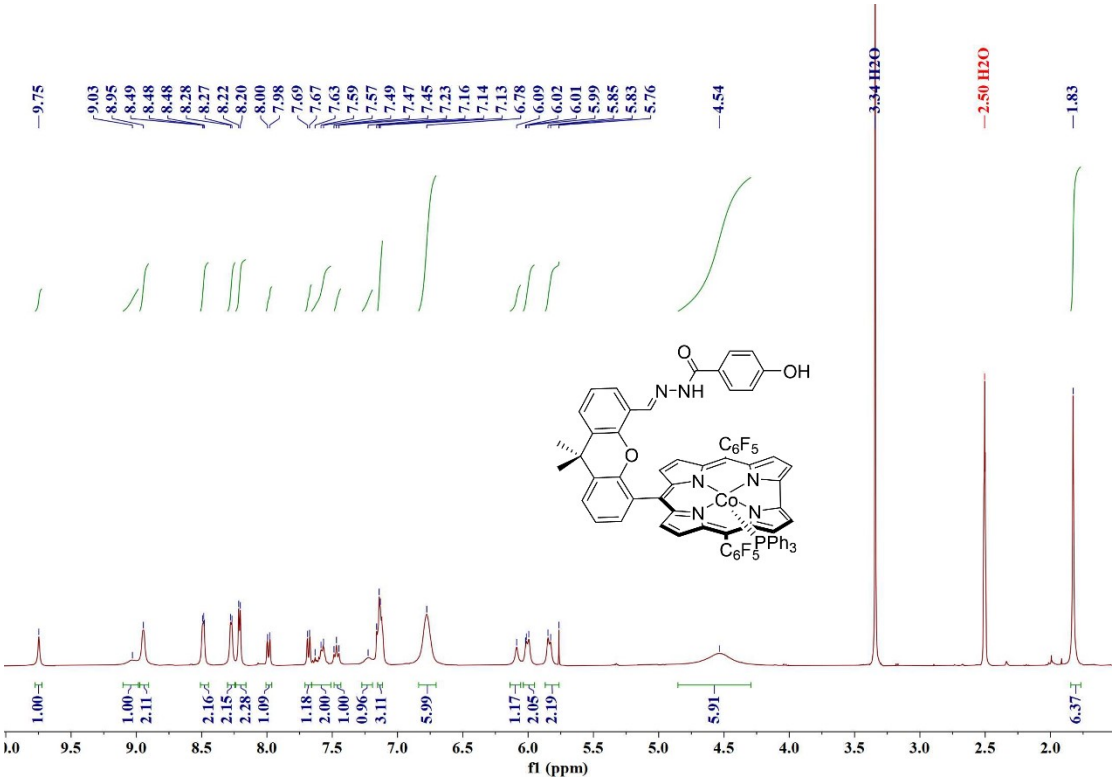

Fig. S4-1 ^{1}H NMR spectrum of **BPXHC-Co(2)**.

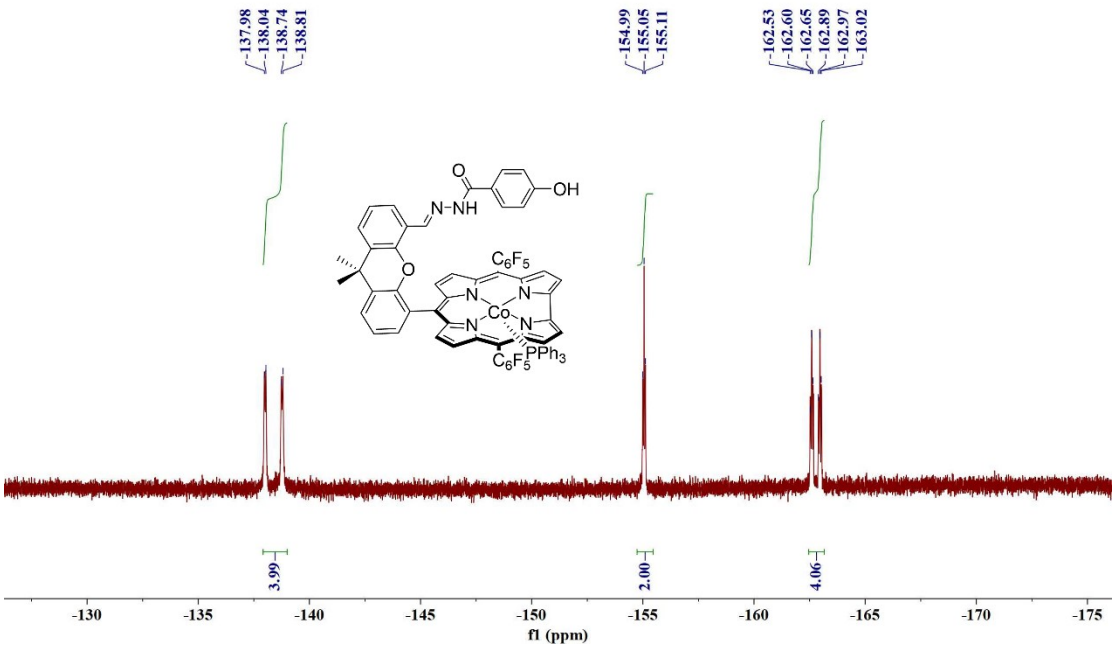

Fig. S4-2 ^{19}F NMR spectrum of **BPXHC-Co(2)**.

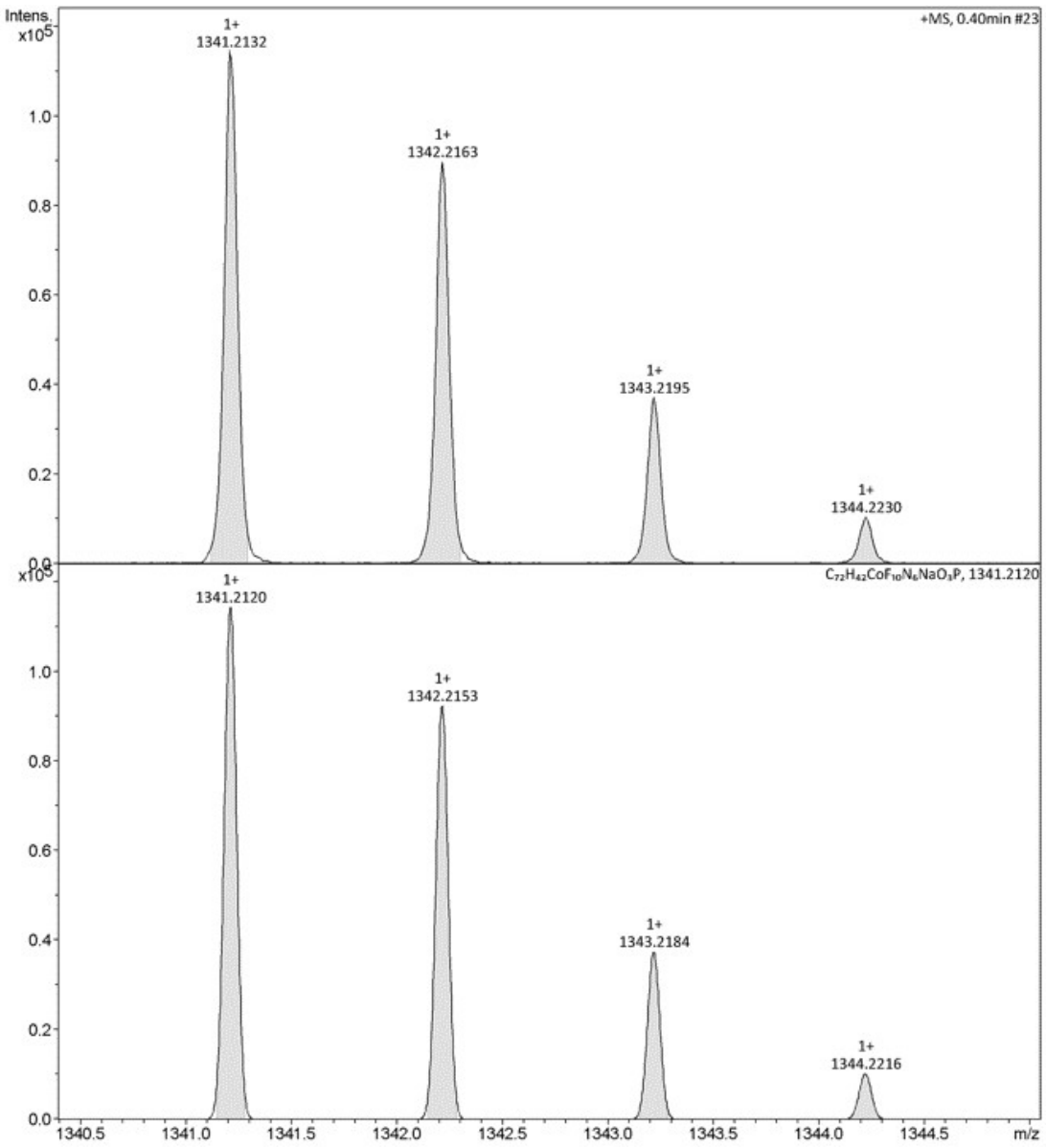

Fig. S4-3 ESI-HRMS spectrum of **BPXHC-Co(2)**.

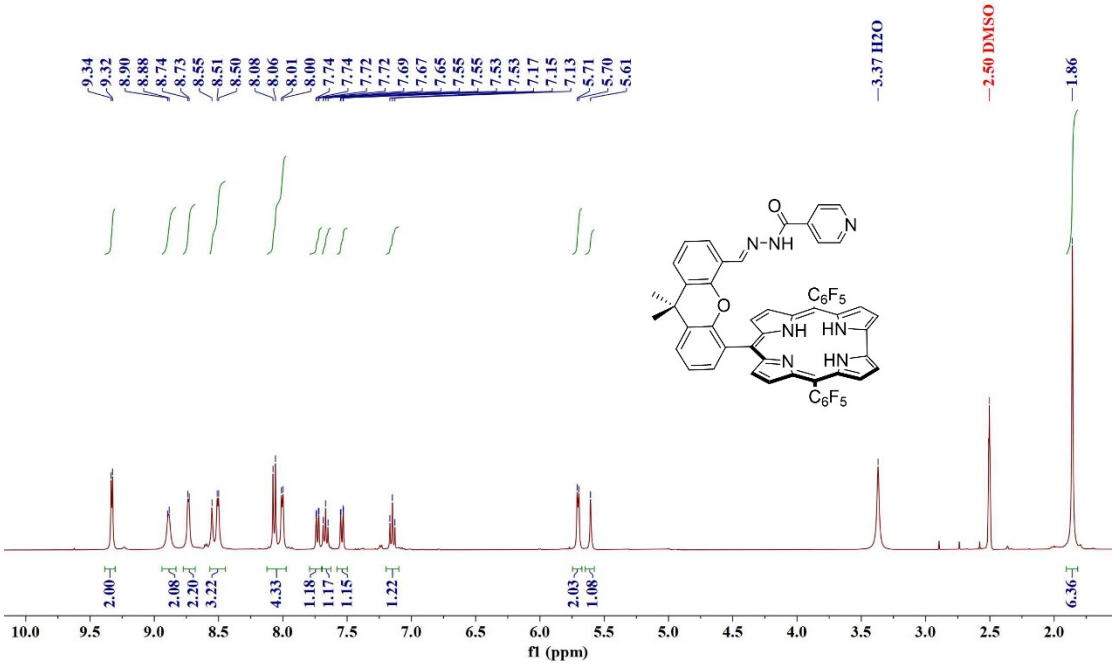

Fig. S5-1 ^{1}H NMR spectrum of **BPXS**

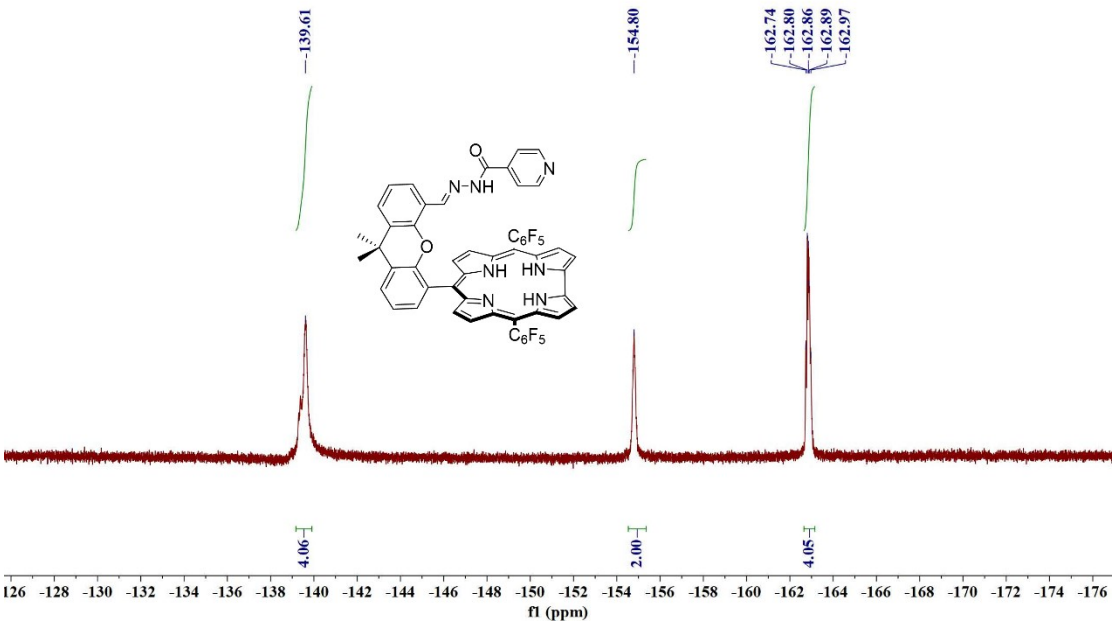

Fig. S5-2 ^{19}F NMR spectrum of **BPXSC.**

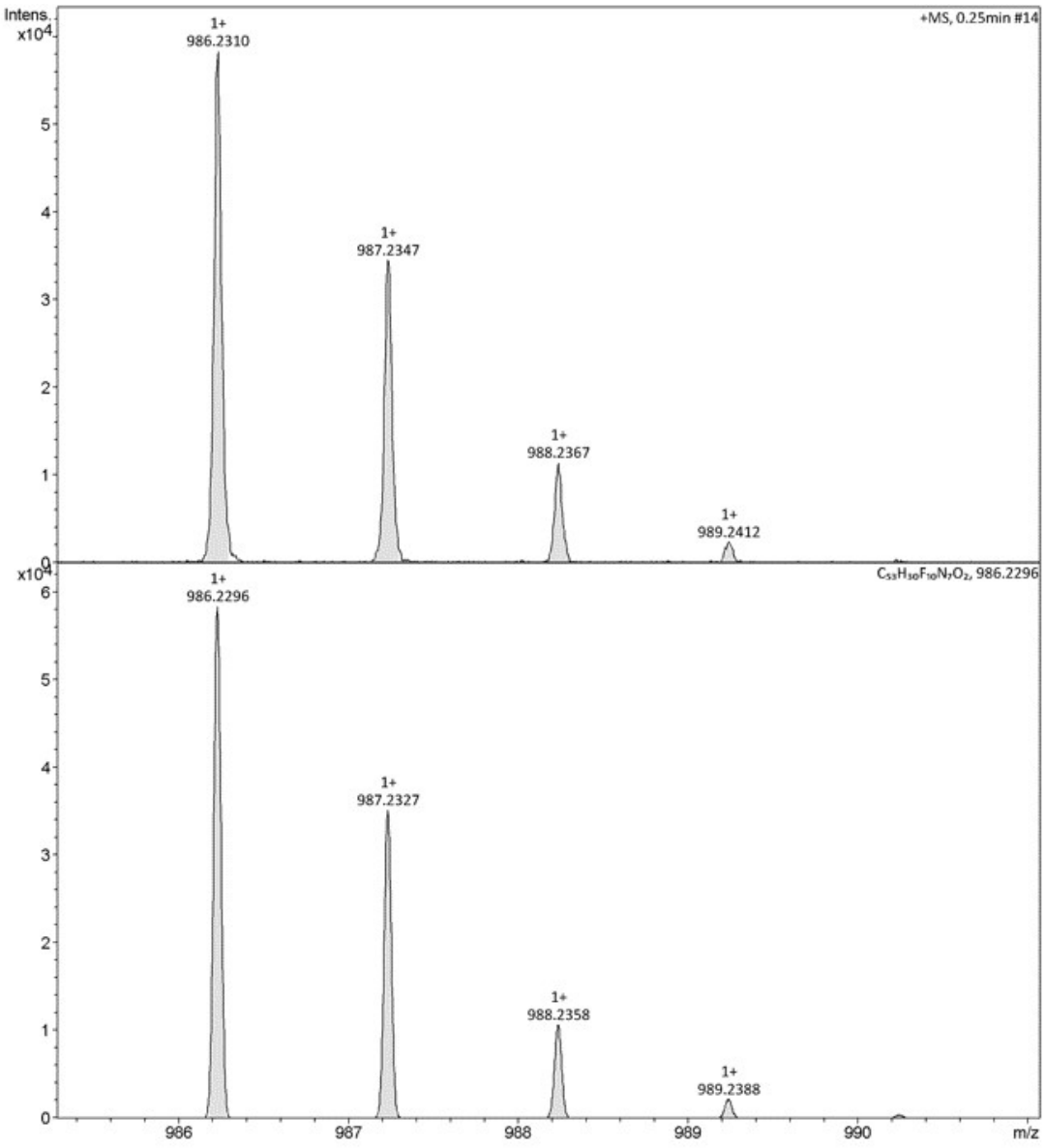

Fig. S5-3 ESI-HRMS spectrum of **BPXSC**

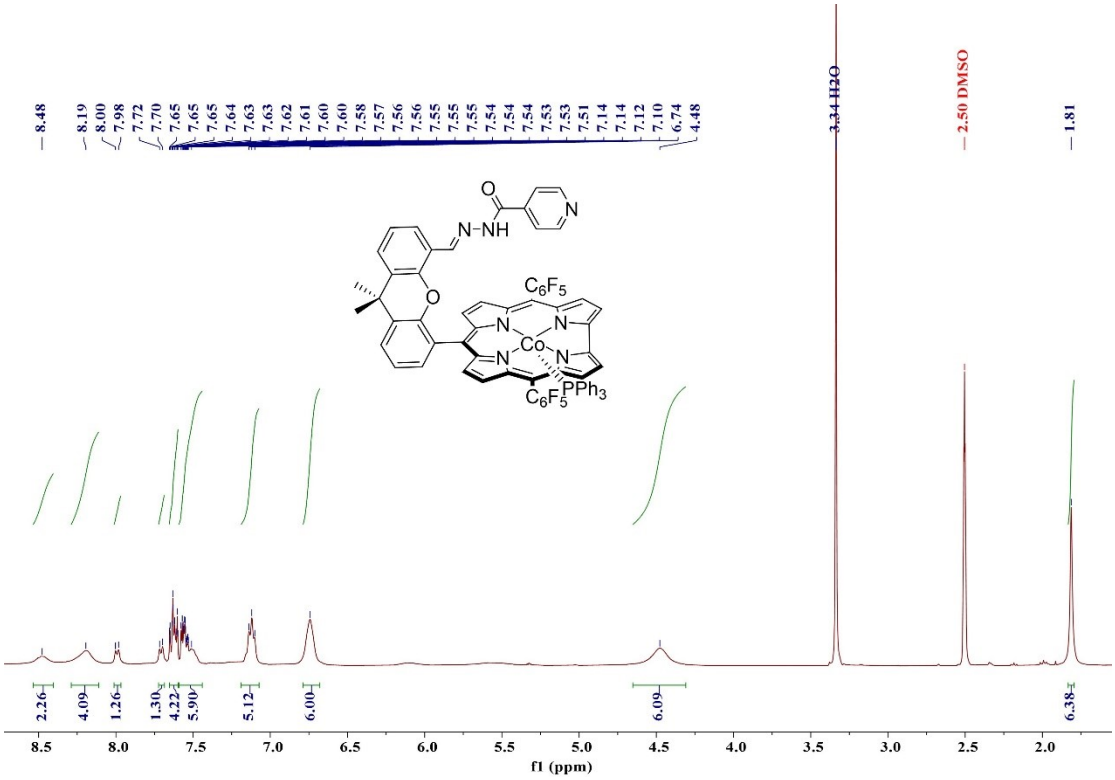

Fig. S6-1 ^{1}H NMR spectrum of **BPXSC-Co(3).**

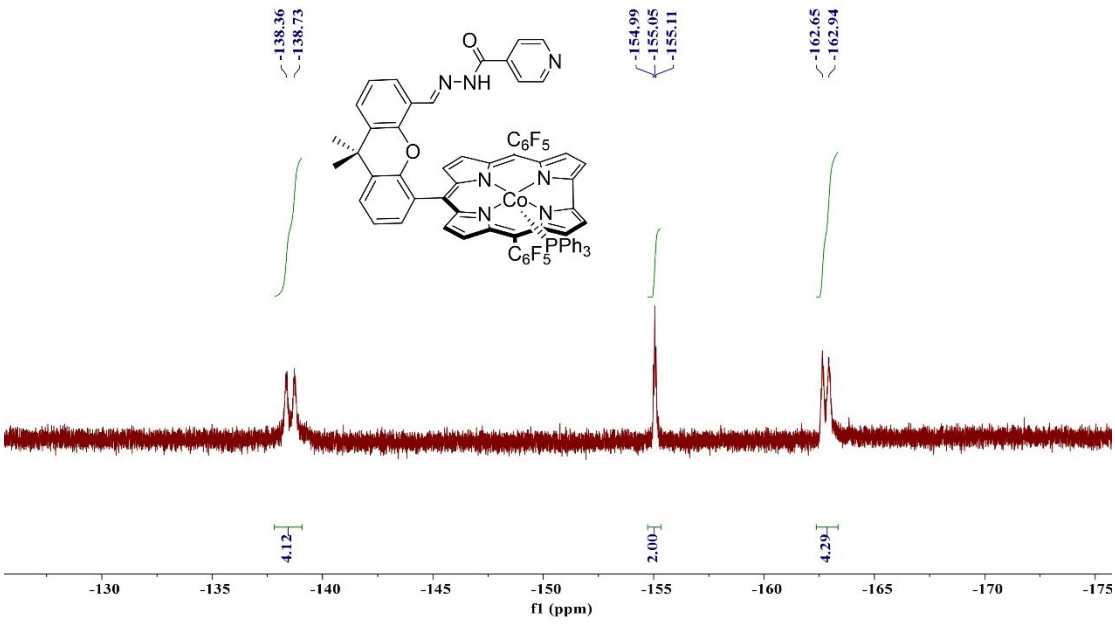

Fig. S6-2 ^{19}F NMR spectrum of **BPXSC-Co(3).**

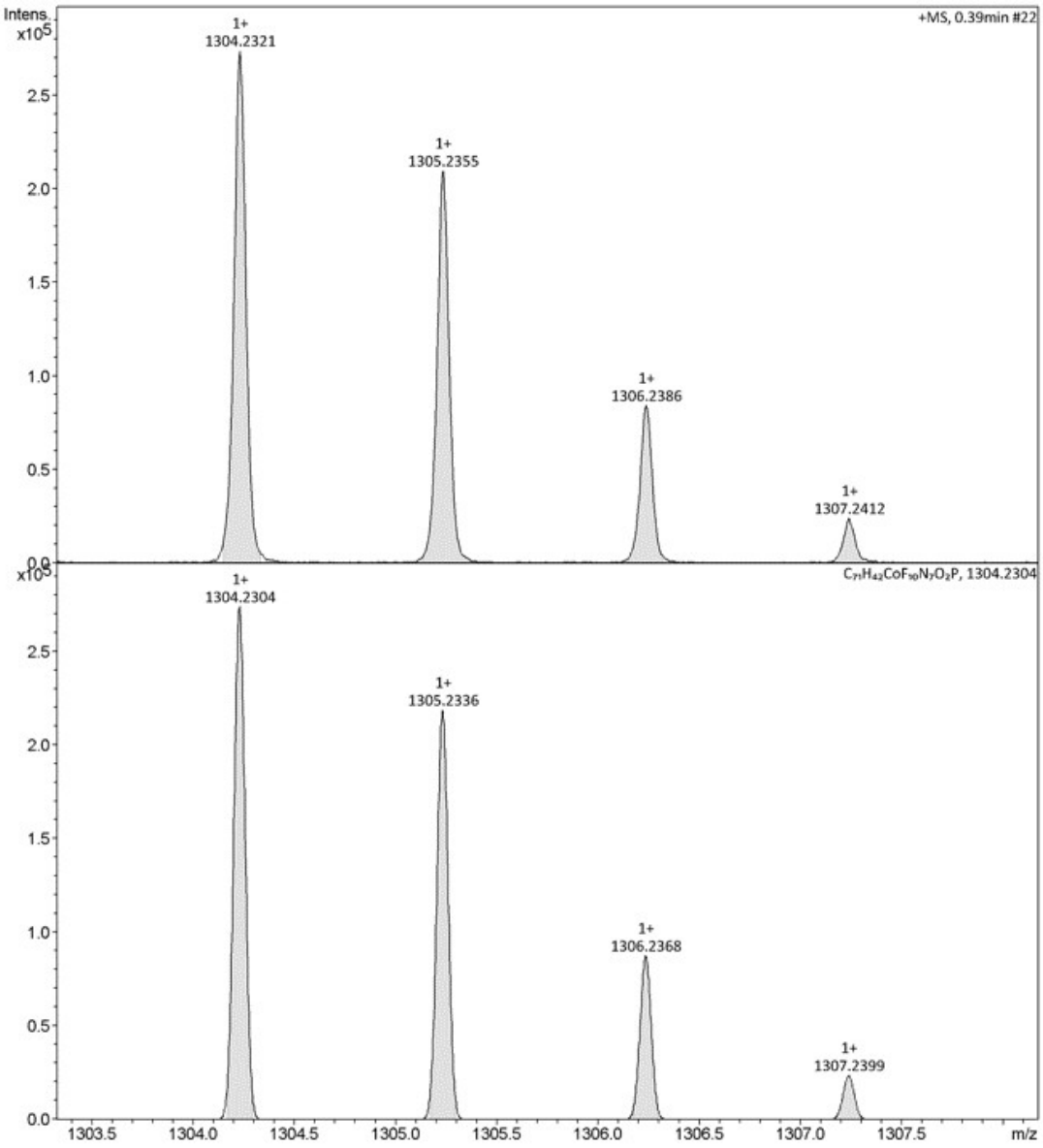

Fig. S6-3 ESI-HRMS spectrum of **BPXSC-Co(3).**

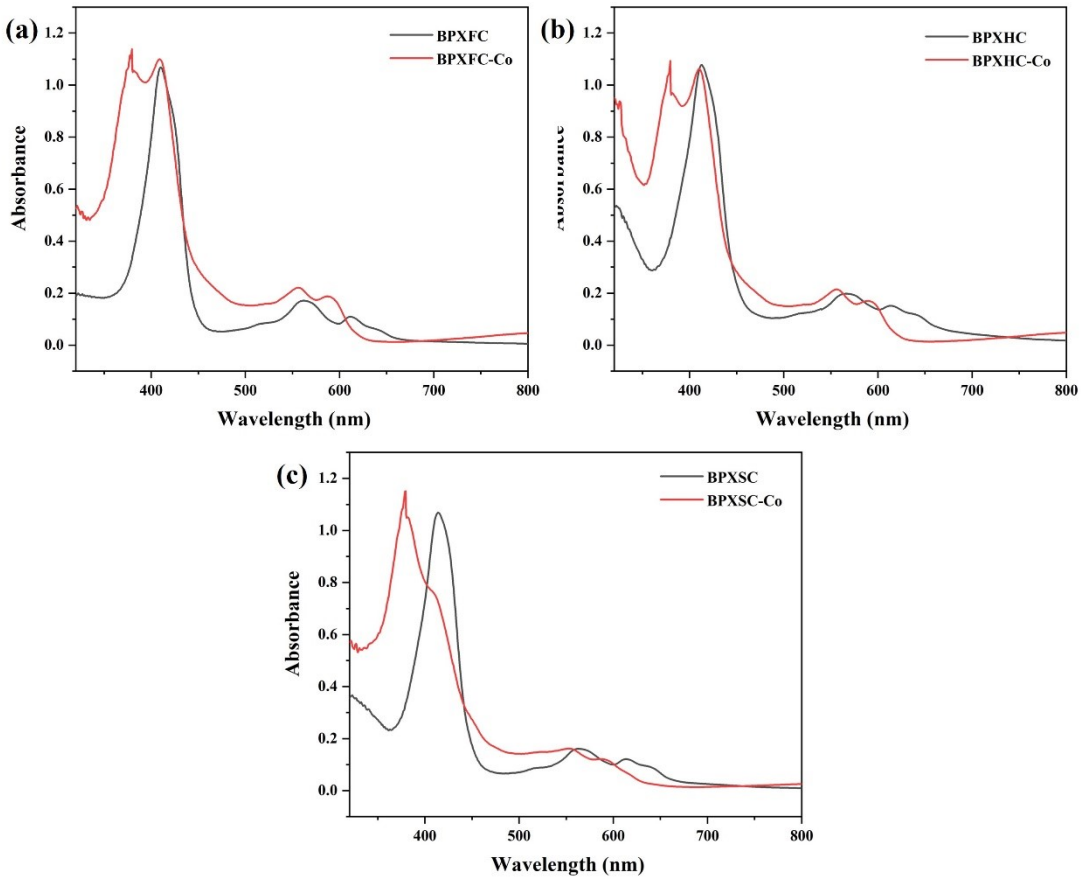

Fig. S7 UV-Vis spectra of BPXFC and BPXFC-Co(**1**) (b) BPXHC and BPXHC-Co**(2)** (c) BPXSC and BPXSC-Co(**3)** in the dichloromethane.

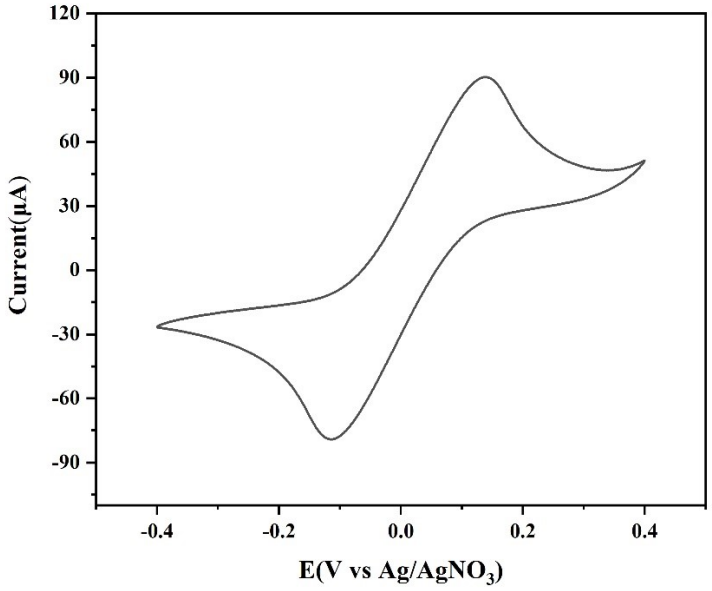

Fig. S8 The redox couple of ferrocene in DMF containing 0.1 M TBAP with blank glassy carbonas the working electrode.

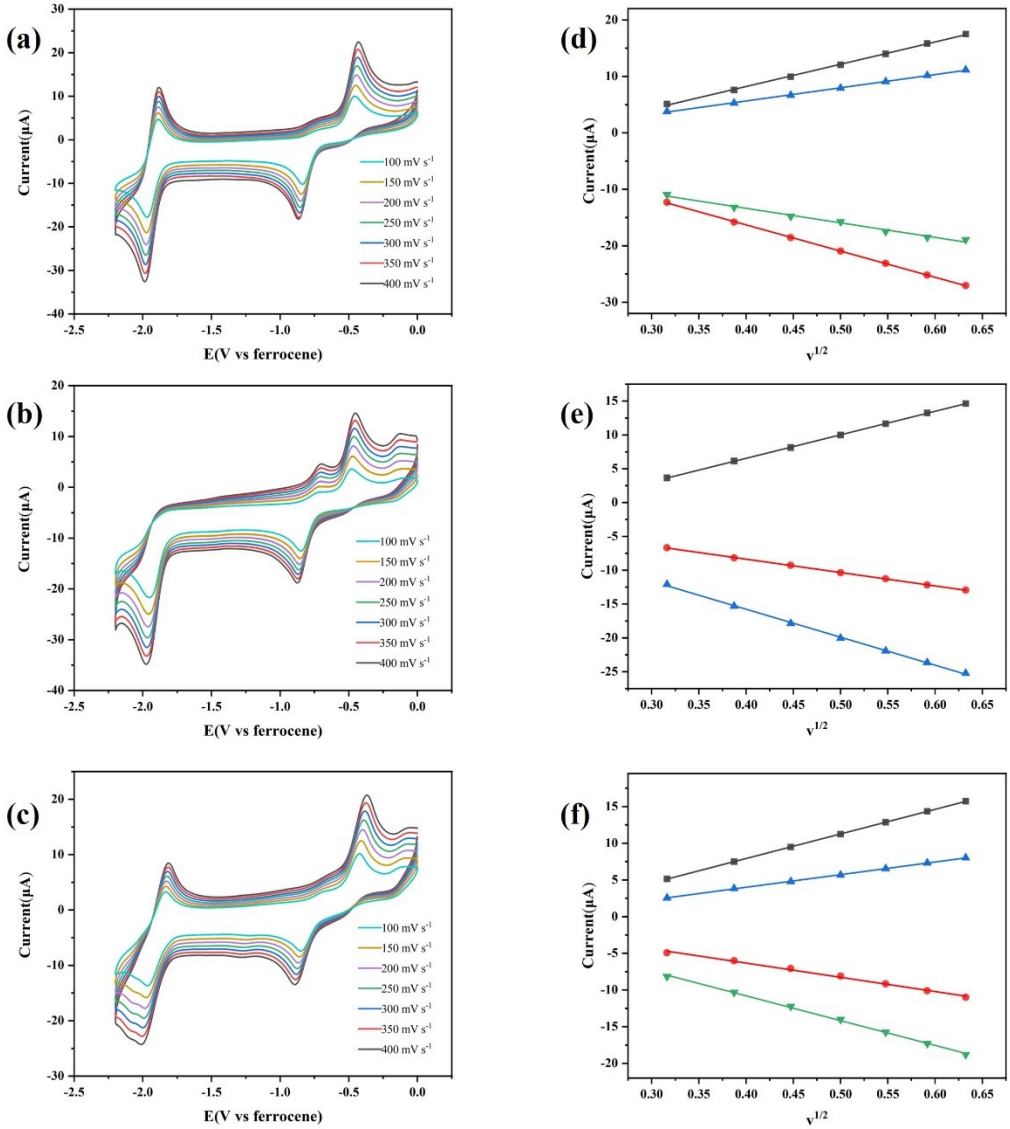

Fig. S9 CVs of 1.0 mM (a)**1**, (b)**2** and (c)**3** with a varying scan rate (v) from 100 mV/s to 400mV/s using the glassy carbon as the working electrode and plots of the maximum current (i_p) for the reduction and oxidation waves *vs*. the scan rate ($v^{1/2}$).

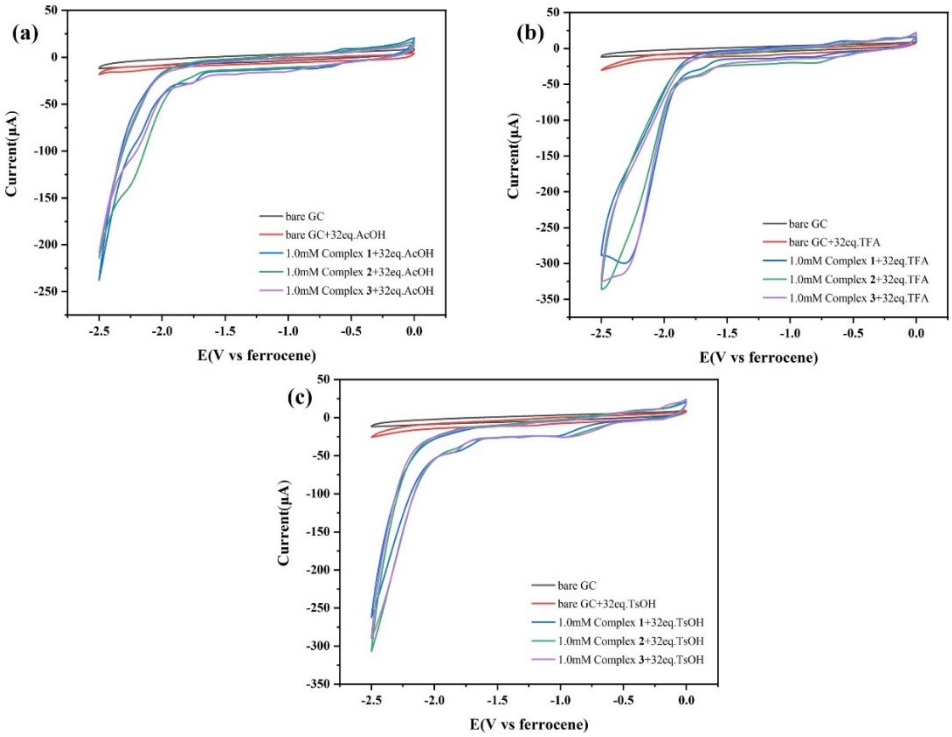

Fig. S10 Comparison of CV test between bare GC and BPXFC-Co(**1**), BPXHC-Co(**2**) and BPXSC-Co(**3**) at high acid concentration.

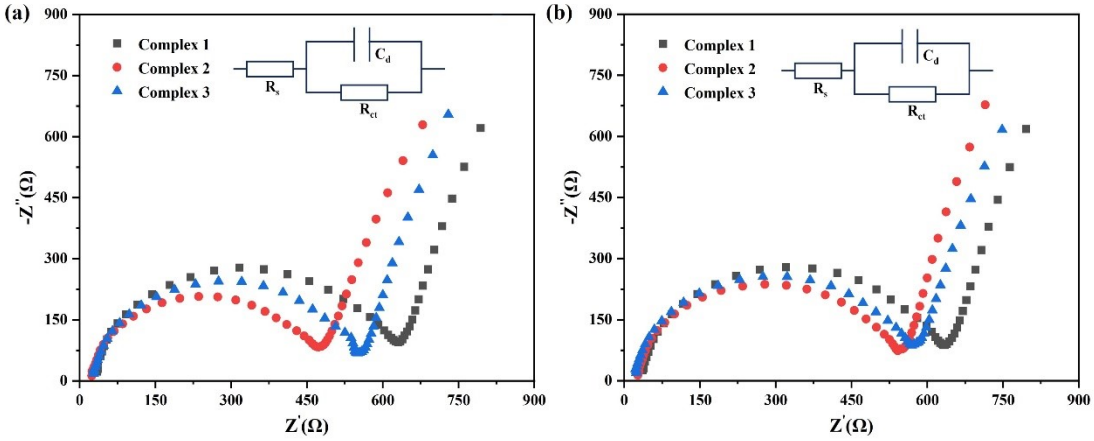

Fig. S11 Nyquist plots of 1.0 mM Co corrole complexes **1**-**3** with 32eq TFA(a) and 32eq TsOH(b) in CH_2Cl_2.

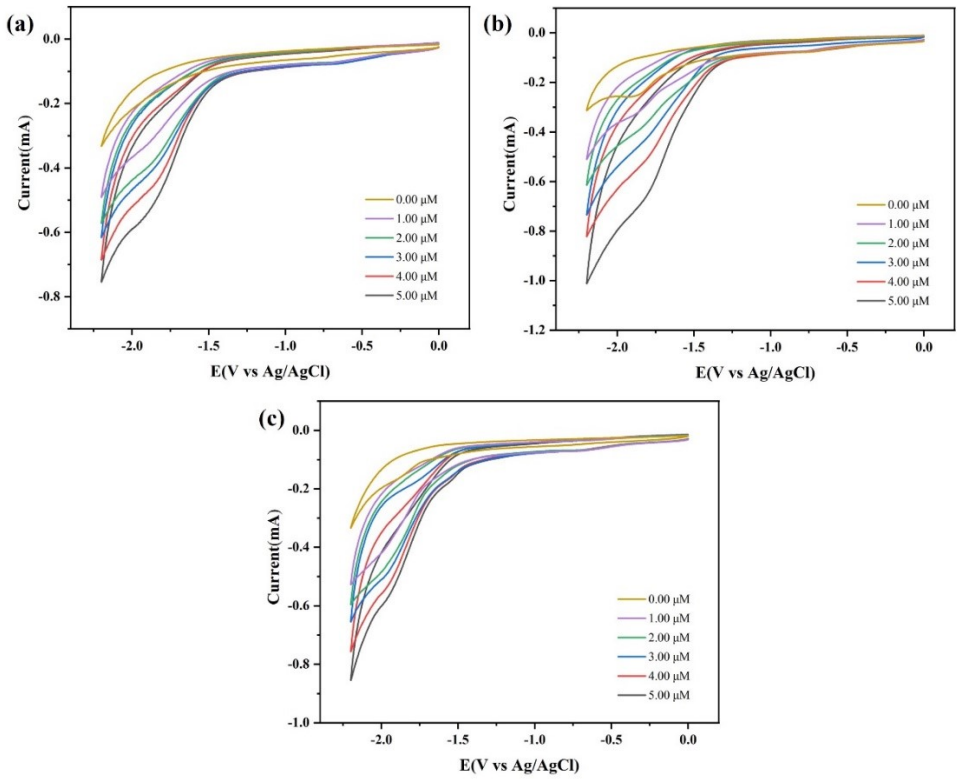

Fig. S12 CVs of various concentrations of complex **1** (a), **2** (b), and **3** (c) in nature aqueous medium using GC as working electrode, carbon rod as counter electrode, and Ag/AgCl a s reference electrode at 0.1 V s^{-1} scan rate.

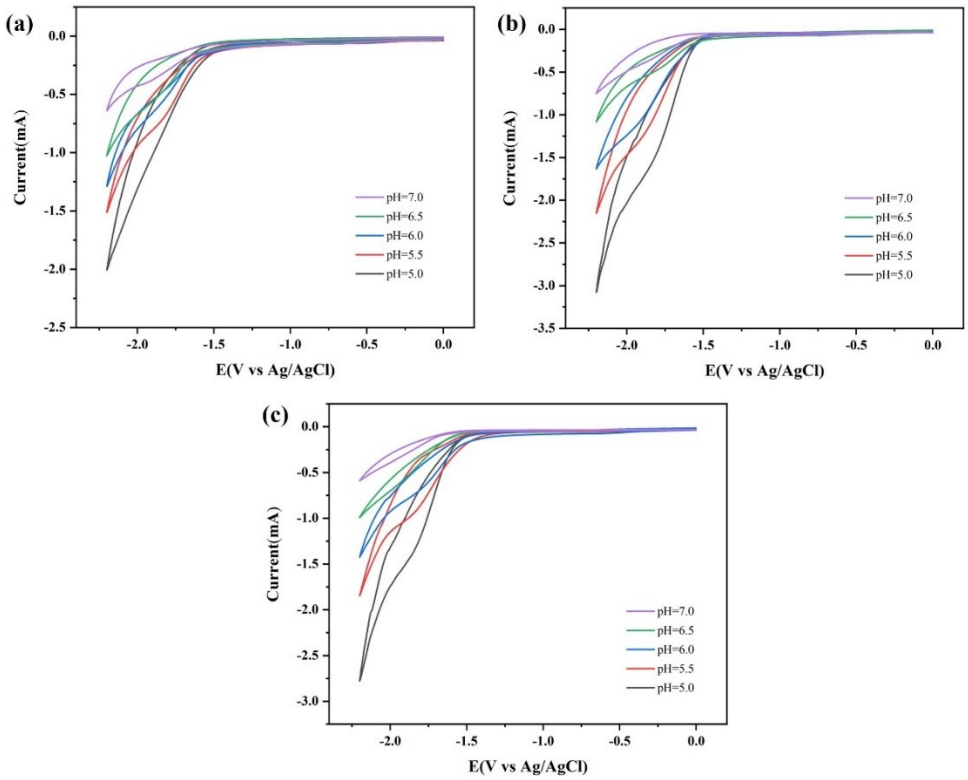

Fig.S13 CVs of 5.0 μM complex **1** (a), **2** (b), and **3** (c) in acetonitrile/water (v/v=2/3) with decreasing pH

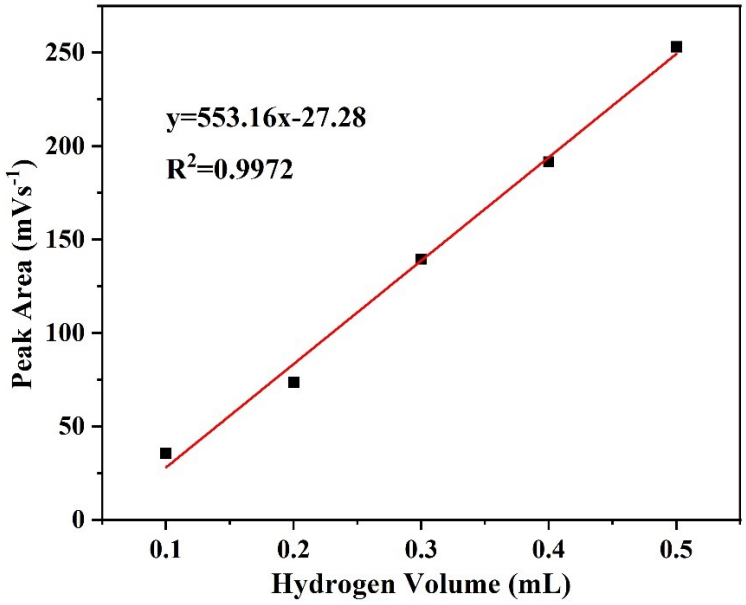

Fig S14. The hydrogen calibration plot from GC measurements.

Table S1. Crystal data of complex **1**.

Identification code	complex 1
Empirical formula	$C_{65}H_{36}CoF_{10}N_4O_2P$
Formula weight	1184.88
Temperature/K	170
Crystal system	monoclinic
Space group	$P2_1/c$
a/Å	8.8638(3)
b/Å	27.6166(10)
c/Å	22.2046(8)
α/°	90
β/°	93.3670(10)
γ/°	90
Volume/Å^3	5426.0(3)
Z	4
ρ_{calc}g/cm^3	1.450
μ/mm^{-1}	0.431
F(000)	2408.0
Crystal size/mm^3	0.15 × 0.08 × 0.05
Radiation	MoKα (λ = 0.71073)
2Θ range for data collection/°	4.712 to 52.796
Index ranges	-9 ≤ h ≤ 11, -34 ≤ k ≤ 33, -27 ≤ l ≤ 27
Reflections collected	32745
Independent reflections	10843 [R_{int} = 0.0522, R_{sigma} = 0.0559]
Data/restraints/parameters	10843/0/750
Goodness-of-fit on F^2	1.053
Final R indexes [I>=2σ (I)]	R_1 = 0.0671, wR_2 = 0.1758
Final R indexes [all data]	R_1 = 0.0911, wR_2 = 0.1928
Largest diff. peak/hole / e Å^{-3}	0.58/-0.34

Table S2. Crystal data of complex **2**.

Identification code	complex 2	c
Empirical formula	$C_{75}H_{49}CoF_{10}N_6O_3P$	C
Formula weight	1362.10	1
Temperature/K	150.00	1
Crystal system	monoclinic	m
Space group	$P2_1/c$	P
a/Å	14.2830(3)	8
b/Å	31.7234(5)	2
c/Å	14.9263(2)	2
α/°	90	9
β/°	114.0410(10)	9
γ/°	90	9
Volume/Å^3	6176.51(19)	5
Z	4	4
ρ_{calc}g/cm^3	1.465	1
μ/mm^{-1}	3.172	0
F(000)	2788.0	2
Crystal size/mm^3	? × ? × ?	0
Radiation	CuKα (λ = 1.54178)	M
2Θ range for data collection/°	5.572 to 130.41	4
Index ranges	$-16 \le h \le 16$, $-37 \le k \le 37$, $-15 \le l \le 17$	-9
Reflections collected	43901	3
Independent reflections	10407 [R_{int} = 0.0964, R_{sigma} = 0.0806]	1
Data/restraints/parameters	10407/0/869	1
Goodness-of-fit on F^2	1.019	1
Final R indexes [I>=2σ (I)]	R_1 = 0.0515, wR_2 = 0.1132	R
Final R indexes [all data]	R_1 = 0.0804, wR_2 = 0.1286	R
Largest diff. peak/hole / e Å^{-3}	0.60/-0.50	0

Table S3. The selected bond distances (Å) for complex **1**

Atom	Atom	Length/Å
Co1	P1	2.2124(12)
Co1	N1	1.869(3)
Co1	N2	1.889(3)
Co1	N3	1.889(3)
Co1	N4	1.868(3)
Co1	O2	5.8510

Table S4. The selected bond distances (Å) for complex **2**

Atom	Atom	Length/Å
Co1	P1	2.2213(9)
Co1	N1	1.861(2)
Co1	N2	1.864(3)
Co1	N3	1.880(2)
Co1	N4	1.881(3)
Co1	N6	5.0220
Co1	O3	7.6150

Table S5. The selected Bond Angles (°) for complex **2**

Atom	Atom	Atom	Angle/°
N1	Co1	P1	99.16(11)
N1	Co1	N2	89.48(13)
N1	Co1	N3	161.37(15)
N2	Co1	P1	100.60(11)
N3	Co1	P1	97.96(11)
N3	Co1	N2	94.55(13)
N4	Co1	P1	97.07(11)
N4	Co1	N1	80.77(14)
N4	Co1	N2	160.98(15)
N4	Co1	N3	89.91(14)

Table S6**.** The selected Bond Angles (°) for complex **2**

Atom	Atom	Atom	Angle/°
N4	Co1	P1	92.41(8)
N4	Co1	N3	81.04(11)
N4	Co1	N2	160.87(11)
N4	Co1	N1	89.66(11)
N3	Co1	P1	91.55(8)
N3	Co1	N2	89.29(11)
N3	Co1	N1	161.85(10)
N2	Co1	P1	104.39(8)
N2	Co1	N1	94.83(11)
N1	Co1	P1	104.46(8)

Table S7 Redox potentials of cobalt complexes in DMF (V vs. ferrrocene) performed by 0.1 M TBAP

Complex	Couple of Co^{III}/Co^{II}		Couple of Co^{II}/Co^{I}	Couple of L/L^{-}
	Ox 1, V	Red 1, V	Red 2, V	Red 3, V
1	-0.52	-0.77	-1.87	-2.39
2	-0.53	-0.78	-1.83	-2.31
3	-0.50	-0.77	-1.86	-2.33

Table S8. Catalytic performance parameters of three metal complexes in TFA system.

Complex	$\mathbf{i_{cat}/i_p}$	**TOF, s^{-1}**	**Efficiency (C.E.)**
1	28.46	157.08	0.89
2	33.62	219.36	1.05
3	32.07	199.57	1.00

Table S9. Catalytic performance parameters of three metal complexes in TsOH system.

Complex	$\mathbf{i_{cat}/i_p}$	**TOF, s^{-1}**	**Efficiency (C.E.)**
1	25.53	126.49	0.80
2	31.39	191.12	0.96
3	30.38	179.04	0.95

Table S10 HER activity for transition metal corroles in organic solvent by using organic acids as proton.

Complex	Proton resource	Solution	TOF(s^{-1})	Reference
1	TFA	DMF	157.08	This work
2	TFA	DMF	219.36	This work
3	TFA	DMF	199.57	This work
PFIC-Cu	TsOH	DMF	138	1
PFEC-Fe	TFA	DMF	13	2
(4-BPFC) Co	TsOH	DMF	93	3
(3-BPSC) Co	TsOH	DMF	187	3
Co (PBHC)	TsOH	DMF	203	4
(m-BPHC)Co	TFA	DMF	61.40	5
(o-BPHC)Co	TFA	DMF	122.68	5
$((CF_3)_4$ -tpfc) Cu	TFA	Acetonitrile	227	6
2-PPh_3	TFA	Acetonitrile	17	7
2-Py	TFA	Acetonitrile	19	7
2-NBPC	TFA	Acetonitrile	17.65	8
$Co(dmg)_2Cl$ (4-ethylamine pyridine)	MES	Acetonitrile	1350	9
$[([15]pydieneN_5)Co(H_2O)_2](ClO_4)_2$ (1-Co)	H_2O	Buffer	2210	10

References

1. L. W. Wu, Y. F. Yao, S. Y. Xu, X. Y. Cao, Y. W. Ren, L. P. Si, H. Y. Liu, B. Mecheri, W. D. Freitas and A. Glisenti, *Catalysts*, 2024, **14**.
2. P. Yadav, I. Nigel-Etinger, A. Kumar, A. Mizrahi, A. Mahammed, N. Fridman, S. Lipstman, I. Goldberg and Z. Gross, *Iscience*, 2021, **24**.
3. A. V. Dolganov, O. Y. Chernyaeva, S. G. Kostryukov, A. V. Balandina, E. O. Solovyova, A. D. Yudina, A. A. Akhmatova and Y. I. Lyukshina, *International Journal of Hydrogen Energy*, 2020, **45**, 501-507.
4. Z. Y. Lv, G. Yang, B. P. Ren, Z. Y. Liu, H. Zhang, L. P. Si, H. Y. Liu and C. K. Chang, *European Journal of Inorganic Chemistry*, 2023, DOI: 10.1002/ejic.202200755.
5. Z. M. Zhu, W. Y. Peng, W. Yang, C. Ling, H. Zhang, L. P. Si and H. Y. Liu, *Applied Organometallic Chemistry*, 2023, **37**.
6. K. Sudhakar, A. Mahammed, Q. C. Chen, N. Fridman, B. Tumanskii and Z. Gross, *Acs Applied Energy Materials*, 2020, **3**, 2828-2836.
7. A. Kumar, S. Fite, A. Raslin, S. Kumar, A. Mizrahi, A. Mahammed and Z. Gross, *Acs Catalysis*, 2023, **13**, 13344-13353.
8. Q.-W. Yan, L.-W. Wu, Z.-W. Liu, F. Chen, C. Ling, H.-Y. Liu, X. Xiao and L.-P. Si, *Green Chemistry*, 2024, DOI: 10.1039/D3GC04884E.
9. D. Dolui, A. Mir and A. Dutta, *Chemical Communications*, 2020, **56**, 14841-14844.
10. J.-W. Wang, K. Yamauchi, H.-H. Huang, J.-K. Sun, Z.-M. Luo, D.-C. Zhong, T.-B. Lu and K. Sakai, *Angewandte Chemie International Edition*, 2019, **58**, 10923-10927.